UNIVERSIDAD REGIONAL AMAZÓNICA IKIAM

FACULTAD DE CIENCIAS DE VIDA

CARRERA DE BIOTECNOLOGÍA

Síntesis de microesferas $Bi_4O_5I_2$ para descontaminación de agua mediante fotocatálisis: degradación de propilparabeno e inactivación de *Escherichia coli*

Proyecto de investigación previo a la obtención del Título de:

INGENIERO EN BIOTECNOLOGÍA

AUTOR: LEONARDO FRANCISCO PROAÑO RHON

TUTOR: Mgs. LUIS MIGUEL QUISHPE QUISHPE

CO-TUTOR: Ph.D MIGUEL HERRERA ROBLEDO

Tena – Ecuador

2024

Carrera de Biotecnología

Declaración de derecho de autor, autenticidad y responsabilidad

Tena, 03 de septiembre de 2024

Yo, Leonardo Francisco Proaño Rhon, con documento de identidad 1720284742, declaro que los resultados obtenidos en la investigación que presento en este documento final, previo a la obtención del título de Ingeniería en Biotecnología, son absolutamente inéditos, originales, auténticos y personales.

En virtud de lo cual, el contenido, criterios, opiniones, resultados, análisis, interpretaciones, conclusiones, recomendaciones y todos los demás aspectos vertidos en el presente documento, son de mi autoría y de mi absoluta responsabilidad.

Firmado electrónicamente por:
LEONARDO FRANCISCO PROANO RHON

Leonardo Francisco Proaño Rhon

CI: 1720284742

Carrera de Biotecnología

Autorización de publicación en el repositorio institucional

Tena, 03 de septiembre de 2024

Yo, Leonardo Francisco Proaño Rhon, con documento de identidad 1720284742 en calidad de autor/a y titular de los derechos morales y patrimoniales del trabajo de titulación "Síntesis de microesferas $BI_4O_5I_2$ para descontaminación de agua mediante fotocatálisis: degradación de propilparabeno e inactivación de *Escherichia coli*.", de conformidad con el Art. 114 del CÓDIGO ORGÁNICO DE LA ECONOMÍA SOCIAL DE LOS CONOCIMIENTOS, CREATIVIDAD E INNOVACIÓN, reconozco a favor de la Universidad Regional Amazónica Ikiam una licencia gratuita, intransferible y no exclusiva para el uso no comercial de la obra, con fines estrictamente académicos.

Así mismo autorizo a la Universidad Regional Amazónica Ikiam para que realice la publicación de este trabajo de titulación en el Repositorio Institucional de conformidad a lo dispuesto en el Art. 144 de la Ley Orgánica de Educación Superior.

Atentamente,

Firmado electrónicamente por:
LEONARDO FRANCISCO PROANO RHON

Leonardo Francisco Proaño Rhon

CI: 1720284742

Carrera de Biotecnología

Certificado de dirección de trabajo titulación

Tena, 03 de septiembre de 2024

Certifico que el trabajo de titulación: "Síntesis de microesferas $BI_4O_5I_2$ para descontaminación de agua mediante fotocatálisis: degradación de propilparabeno e inactivación de *Escherichia coli*", aprobado bajo el mecanismo de titulación de: artículo, fue realizado por Leonardo Francisco Proaño Rhon, bajo mi dirección.

El mismo ha sido revisado en su totalidad y analizado por la herramienta de verificación de similitud de contenido; por lo tanto, cumple con los requisitos teóricos, científicos, técnicos, metodológicos y legales establecidos por la Universidad Regional Amazónica Ikiam, para su entrega y defensa.

Firmado electrónicamente por:
LUIS MIGUEL QUISHPE QUISHPE

Luis Miguel Quishpe Quishpe

CI: 1500843048

Tutor

Firmado electrónicamente por:
MIGUEL HERRERA ROBLEDO

Miguel Herrera Robledo

CI: 1550516452

Cotutor

AGRADECIMIENTOS

Agradezco a mis padres y familia, que ha sido un pilar fundamental en mi desarrollo personal. A mis tías Jisela y Fernanda Rhon, quienes siempre me apoyaron de forma incondicional durante mis estudios en Ikiam. A Maria José Auquilla, por escucharme, apoyarme y motivarme a siempre ser el mejor.

También agradezco a Michael Zuarez, Luis Miguel Quishpe y Miguel Herrera por ser los tutores más excepcionales, profesionales y humanos que he conocido. Además, agradezco a las técnicas de laboratorio Andrea Salgado, Carolina Ñacato y Giovanna Morán por su apoyo en mi trabajo de titulación.

Finalmente, agradecer al proyecto "Nature-based living lab for interdisciplinary practical and research semester on sustainable development and environmental protection in the amazon rainforest" por financiar el desarrollo de mi trabajo de titulación.

DEDICATORIA

Dedico este trabajo a mi abuela Yeya y a mis tíos Francisco y Jaime Humberto, quienes me brindaron su apoyo incondicional y consejos durante mis estudios, aunque ya no están con nosotros.

TABLA DE CONTENIDO

ÍNDICE DE TABLAS

ÍNDICE DE FIGURAS

RESUMEN

La degradación de contaminantes del agua como el propilparabeno (PP) y la inactivación de bacterias patógenas como *Escherichia coli* se ha convertido en un reto. Por lo tanto, se sintetizaron microesferas en forma de flor de $Bi_4O_5I_2$ mediante un método solvotermal y de calcinación para la degradación e inactivación de contaminantes del agua y patógenos, respectivamente. Las microesferas de $Bi_4O_5I_2$ se caracterizaron por difracción de rayos X (DRX), microscopía electrónica de barrido (MEB) y espectroscopía de energía dispersiva de rayos X (EED). Los patrones de DRX de la muestra calcinada estaban bien alineados con la fase monoclínica de $Bi_4O_5I_2$. La composición elemental por EED mostró que la muestra era similar a la fórmula teórica $Bi_4O_5I_2$. Las microesferas en forma de flor de $Bi_4O_5I_2$ mostraron una excelente actividad fotocatalítica en la degradación del PP y la inactivación de células de *E. coli*. Por lo tanto, estos resultados sugieren que las microesferas con forma de flor de $Bi_4O_5I_2$ podrían ser un candidato potencial para el tratamiento del agua debido a su alta actividad fotocatalítica.

Palabras Clave

Escherichia coli, Fotocatálisis, Microesferas $Bi_4O_5I_2$, Propilparabeno

ABSTRACT

The degradation of water pollutants such as propylparaben (PP) and the inactivation of pathogenic bacteria as *Escherichia coli* has become a challenge. Therefore, $Bi_4O_5I_2$ flower-like microspheres were synthesized by a solvothermal/calcination method for the degradation and inactivation of waterborne pollutants and pathogens, respectively. $Bi_4O_5I_2$ microspheres were characterized by X-ray diffraction (XRD), scanning electron microscopy (SEM) and energy-dispersive X-ray spectroscopy (EDS). The XRD patterns of the calcinated sample were well aligned to the monoclinic phase of $Bi_4O_5I_2$. The elemental composition by EDS showed that the sample was similar to the theorical formula $Bi_4O_5I_2$. The $Bi_4O_5I_2$ flower-like microspheres exhibited an excellent photocatalytic activity in the degradation of PP and inactivation of *E. coli* cells. Therefore, these results suggest that $Bi_4O_5I_2$ flower-like microspheres could be a potential candidate for water treatment due to their high photocatalytic activity.

Keywords

$Bi_4O_5I_2$ microspheres, *Escherichia coli*, Photocatalysis, Propylparaben.

Journal of Environmental Chemical Engineering

Link: Guide for authors - Journal of Environmental Chemical Engineering - ISSN 2213-3437 | ScienceDirect.com by Elsevier

Synthesis of $Bi_4O_5I_2$ microspheres for water decontamination by photocatalysis: degradation of propylparaben and inactivation of *Escherichia coli*

Leonardo Proaño-Rhon[a]

[a]Universidad Regional Amazónica Ikiam, Muyuna Road km 7, San Juan de Tena, Napo, Ecuador.

1. INTRODUCTION

Water supplies around the world have been affected by the presence of endocrine disrupting chemicals (EDCs) and pathogenic bacteria. On the one hand, EDCs interfere with the synthesis of endocrine hormones, their biological actions, metabolism and alter hormone-regulated homeostatic processes in many tissues and physiological systems [1,2]. Among the EDCs, propylparaben (PP) has stood out because is one of the most widely used chemicals in food preservation, pharmaceuticals and cosmetics [2–4]. In this sense, it has been reported PP concentrations of 2.4-144 ng L^{-1} in lakes and rivers [5] and, 2.46-14.9 µg L^{-1} in sewage water [6].Due to these facts, the skin and oral exposure to PP has increased the prevalence of breast cancer, decreased sperm production and testosterone levels [7–9]. On the other hand, the presence of waterborne pathogenic bacteria is a global concern due to the emergence of antibiotic-resistant bacteria (ARB) [10–12]. The World Health Organization has recognized *Escherichia coli* (*E. coli*) as one of the most persistence ARB [11] and responsible for the majority of diarrhea cases reported in developing countries [13]. For example, some pathotypes of *E. coli* like enteropathogenic (EPEC), uropathogenic (UPEC) and enterohemorrhagic (EHEC), among others, can cause damage to different tissues (e.g., bloodstream and urinary tract) and produce major clinical manifestations [11,14,15]. In this sense, in order to ensure the public health, it is important to develop processes or technologies able to degrade PP and inactivate *E. coli*.

Currently, there are some processes for the removal of PP [16,17] and inactivation of *E. coli* [18,19]. For the removal of PP from water, biodegradation, physical and advanced chemical oxidation processes have been reported [17]. However, PP removal with physical methods or advanced chemical oxidation is very expensive, while biodegradation generates toxic by-products [17]. Although, disinfection methods such as chlorination and ozonation have been reported to be hazardous to human health due to the production of toxic by-products [18]. While disinfection by UV irradiation do not completely inactivate bacteria due to cellular repair mechanisms [19,20]. Due to these

facts, in recent years has been developed new eco-friendly and efficient water treatment processes such as photocatalysis [21,22]. Photocatalysis is an advanced oxidation process (AOP) which requires a semiconductor material (i.e., photocatalyst) that absorbs photons from the light (e.g., visible or UV) with an energy higher or equal to its band gap energy [23]. The absorption of photons by the semiconductor results in the excitation of electrons (e^-) from the valence band (VB) to the conduction band (CB), leaving a vacancy (i.e., a hole (h^+)) with positive charge in the VB [24]. Consequently, the e^- and h^+ migrate to the surface of semiconductor and react with electron-acceptor (e.g., O_2) and electron-donor molecules (e.g., H_2O) [23], generating reactive oxygen species (ROS) [22]. At present, TiO_2 is one of the most widely used photocatalytic materials [25]. However, TiO_2 can only work with UV light because its band gap is wider than 3.2 eV [26]. Owing to this, its efficiency with sunlight is low, since the solar spectrum has only 4% UV light [27]. Due to these facts, it has been developed semiconductors that work with visible light (i.e., 43% of solar spectrum), such as bismuth-rich bismuth oxyiodide semiconductors ($Bi_xO_yI_z$).

The $Bi_xO_yI_z$ semiconductors stand out due to their excellent electronic and optical properties [25]. It has been reported that the band gap of $Bi_xO_yI_z$ range from 2.0 to 3.0 eV, which allows them to work efficiently with visible light [25]. Furthermore, $Bi_xO_yI_z$ semiconductors have a wider band gap than normal BiOI photocatalysts, which means their redox potentials of the valence and conduction band are more suitable for ROS production. Due to these properties, $Bi_xO_yI_z$ micro/nanostructures have been developed through hydrothermal alkalinization and calcination methods [25]. For example, it has been synthesized $Bi_4O_5I_2$ microbars by a hydrothermal method with a high capacity to degrade bisphenol A [28]. As well as, flower-like $Bi_4O_5I_2/Bi_5O_7I$ nanocomposites have been fabricated to degrade PP [29] and $Bi_4O_5I_2$ nanosheets to inactivate *E. coli* [30]. On the other hand, $Bi_7O_9I_3$ and Bi_5O_7I microspheres have been synthesized by a calcination method for the degradation of tetracycline and rhodamine B, and for nitrogen fixation, respectively [31]. In this sense, studies suggests that the calcination method can enhance the photocatalytic performance by increasing the crystallinity, crystallite size, and active sites of the semiconductor material [25,31,32]. Nevertheless, to date, it has

not been reported the synthesis of $Bi_4O_5I_2$ flower-like microspheres by a solvothermal/calcination method and their photocatalytic efficiency against PP and *E. coli*.

Therefore, this work aims to (1) synthesize $Bi_4O_5I_2$ flower-like microspheres by a solvothermal method, followed by calcination, and characterize them by using a set of instrumental techniques, (2) degrade PP and, (3) Inactivate *E. coli* in solution by using $Bi_4O_5I_2$ photocatalytic microspheres.

2. MATERIAL AND METHODS

2.1. Materials

Bismuth nitrate pentahydrate (Bi $(NO_3)_3 \cdot 5H_2O$), potassium iodide (KI), propylparaben (PP) and ethylene glycol (EG) were of analytical grade and used as received from Sigma-Aldrich (St. Louis, MO, USA). Sodium chloride was of analytical grade and used as received from Panreac (Barcelona, Spain). All the chemicals were used without further purification.

2.2. Synthesis of $Bi_4O_5I_2$ flower-like microspheres

$Bi_4O_5I_2$ microspheres were obtained by calcinating BiOI flower-like microspheres previously synthetized by an adaptation of the temperature and reaction time of the solvothermal method reported by Zuarez-Chamba and coworkers [33]. The BiOI synthesis process was as follows: a solution A was prepared by dissolving 3 mmol (1.455 g) of Bi $(NO_3)_3 \cdot 5H_2O$ in 30 mL of EG with sonication for 30 min, and then under constant stirring (500 rpm) for 30 min. At the same time, a solution B was prepared by dissolving 3 mmol of KI in 30 mL of EG under continuous stirring (500 rpm). Then, solution B was added drop by drop (1 mL min^{-1}) to solution A under constant stirring (500 rpm). The mixed solution was let under constant stirring (500 rpm) for 30 min and, after it was transferred to a 100 mL Teflon-lined Autoclave. The autoclave was placed in a stainless-steel reactor and heated in an oven at 160 °C for 3 h. The precipitate was allowed to cool at room temperature, collected by vacuum filtration and washed first with deionized water, followed with ethanol, and again once with deionized water. The precipitate obtained was dried at 60 °C for 4 h. Finally, the obtained BiOI powder was calcinated in a muffle furnace at 410 °C for 30 min to obtain $Bi_4O_5I_2$ flower-like microspheres.

2.3. Characterization of $Bi_4O_5I_2$ microspheres

The crystalline structure of $Bi_4O_5I_2$ microspheres was characterized by X-ray diffraction (XRD) on a Malvern Panalytical Empyrean X-ray diffractometer equipped with a copper X-ray tube (Kα radiation, λ = 1.54056 A°). XRD data was collected in the 2Θ range between 5° to 90° with a scan rate of 0.017° at 45 kV, and 40 mA. The morphology was observed by scanning electron microscopy (SEM) on a Tescan Mira 3 scanning electron microscope. SEM images and software Image J were used to determine the diameter of the $Bi_4O_5I_2$ microspheres. The elemental chemical composition of the microspheres was determined by energy dispersive X-ray spectroscopy (EDS) using a Bruker X-Flash 6-30 detector coupled to SEM equipment, with a resolution of 123 eV at Mn Kα.

2.4. Degradation of propylparaben

The evaluation of the photocatalytic activity of $Bi_4O_5I_2$ microspheres in the degradation of PP under visible light was performed with a photoreactor equipped with two fans, a 600 mL beaker, a stirring plate, and a white light LED lamp (LEDEX B4665, 50 W, 5000 Lm, 6000 K daylight, 100-200 V) placed 26 cm from the beaker. In this context, a photolysis experiment was performed to identify the photosensitivity of PP. Then, the assay was performed in triplicate as seen in **Table 1**. First, 100 mg of $Bi_4O_5I_2$ powder (photocatalyst dosage = 0.2857 g L^{-1}) was added in 350 mL of a PP solution (5 mg L^{-1}) and dispersed by sonication for 10 min. Then, the solution was stirred at 300 rpm in the dark for 1 h to achieve the adsorption-desorption equilibrium between the contaminant and the photocatalyst surface. Next, the solution was stirred for 3 h in the presence of visible light. Aliquots of 26 mL were taken every 20 min and, then the PP concentration was determined by with a UV-Vis spectrophotometer (Shimadzu) at 255 nm, and using the next equation (1) from the calibration curve (Fig. S1):

$$y = 0.0796x + 0.007 \quad (1)$$

In addition, all reaction conditions like photocatalyst dosage, initial PP concentration,

and stirring speed were kept constant during the assays.

Table 1. Experimental design for the degradation of PP using $Bi_4O_5I_2$ microspheres.

Type of assay	Exposure without light (60 min)	Light exposure (180 min)
PP without photocatalyst	3x	3x
PP with photocatalyst	3x	3x

2.5. Inactivation of *Escherichia coli*

2.5.1. Bacteria culture and preparation

Escherichia coli ATCC 25922™ was cultured in Mueller Hinton Broth (MHB) during 18 to 24 h at 37 °C, with shaking at 150 rpm. Then, 0.5 mL of the bacterial culture was inoculated into sterile MHB. It was incubated at 37 °C with shaking for 90 min to reach bacterial cells in exponential phase bacterial growth (OD 0.4). *E. coli* cells were collected by centrifugation at 4000 rpm for 15 min. After centrifugation, the MHB was discarded, and the pellet was washed two times with NaCl 0.9 % (m/v) solution. In the last wash, the saline solution was discarded, and the pellet was resuspended with 0.5 mL NaCl 0.9% solution.

2.5.2. Photocatalytic inactivation performance

The inactivation performance of $Bi_4O_5I_2$ microspheres was performed using a photoreactor that consisted in a white LED Lamp (400W, 6500 K), as the visible light source, and a cooling system composed of two fans to remove the heat produced by the lamp. Thus, the inner temperature into the photoreactor was maintained at 25 °C. All glassware and magnetic stir bar were sterilized in an autoclave at 121 °C for 15 min before each photocatalytic inactivation experiment. A 100 mL beaker was used to carry out the photocatalytic experiment. For this, 20 mg of $Bi_4O_5I_2$ microspheres (photocatalytic dosage = 0.4 g L^{-1}) was added in 49.5 mL of NaCl 0.9% solution and the

pH was adjusted to 7.0 with 0.1 M NaOH to ensure the survival of the bacterial strain. Then, the solution was sonicated for 10 min to disperse the photocatalyst. After, the entire pellet of bacterial cells previously washed was added to the solution to complete a volume of 50 mL. The density of viable cells in the solution was approximately $1.75x10^7$ CFU mL^{-1}.

In a typical procedure, the solution was stirred at 300 rpm in dark condition for 30 min to achieve the adsorption–desorption equilibrium between the microspheres and bacteria cells. After that, the suspension was stirred under visible light irradiation for 180 min. Aliquots of 100 µL were taken each 30 min, and serial dilutions were subsequently prepared. The density of viable cells was determined by the plate count method. For this, the cell suspensions from each serial dilution were spread on Mueller Hinton Agar (MHA) using a Digralsky handle, and then incubated at 37 °C for 24 h. Finally, the number of colonies formed were counted to obtain the bacterial density (CFU mL^{-1}). The negative control consisted of a bacterial suspension ($1x10^7$ CFU mL^{-1}) in NaCl 0.9% solution, the pH was adjusted to 7.0 with 0.1 M NaOH, and exposed to the same conditions as the photocatalyst assay. Two replicates were made for each serial dilution and each assay was performed in triplicate (**Table 2**).

Table 2. Experimental design of the photocatalytic inactivation of *E. coli* by $Bi_4O_5I_2$ microspheres.

Type of assay	**Exposure without light (30 min)**	**Light exposure (180 min)**
Negative control	3x	3x
Photocatalyst and *E. coli*	3x	3x

3. RESULTS AND DISCUSSION

3.1. Instrumental Characterization

Fig. 1 shows the XRD patterns of the powder and the International Centre for Diffraction Data (ICDD) card No. 98-041–2590 of $Bi_4O_5I_2$. All the diffraction peaks of the crystalline structure of the powder sample correspond to the monoclinic phase of $Bi_4O_5I_2$ with spatial group P 1211, lattice constants a= 15.008 Å, b= 5.696 Å, c= 11.306 Å and β= 100.503 ° [34], and crystallite size of 36.16 nm. The diffraction peaks placed at 2θ: 9.253°, 23.296°, 28.733°, 31.416°, 36.72°, 42.35°, 44.98°, 49.15°, 54.274° , 59.695° and 65.492° are indexed to the crystalline planes (1 0 -1), (3 1 0), (4 1 -1), (4 0 2), (-4 0 4), (3 2 -3), (4 2 2), (0 0 6), (8 1 1), (8 2 -2) and (8 0 4), respectively [35]. Also, the strong intensity and sharpness of the diffraction peaks reveals that $Bi_4O_5I_2$ microspheres are highly pure and crystalline. These results are similar to the reported for other $Bi_4O_5I_2$ semiconductor materials [28,29,35].

However, the $Bi_4O_5I_2$ flower-like microspheres reported in this work exhibit a higher crystallinity and a bigger crystallite size than the other materials mentioned above, which suggests it might have a more efficient charge carrier separation [25]. Furthermore, the high intensity of the (4 1 -1) and (4 0 2) indicates that this semiconductor crystallizes preferentially on these planes. This can be related to an oriented crystallization of $Bi_4O_5I_2$ nanoplates [36,37] on the surface of the microspheres, as seen in the SEM images depicted in the Fig. 2a-b. Then as is observed, the sample is composed by microspheres with an average diameter of about 1.282 ± 0.017 μm, which are decorated by nanoplates of an average thickness of 13.522 ± 0.1 nm. Therefore, these microspheres could have an increased photocatalytic performance compared to smooth microspheres due to the porosity formed by the nanoplates, which allows them to have a larger surface area and more active sites to conduct photocatalytic reactions [38,39]. On the other hand, according to EDS elemental mapping (Fig. 2c-f), Bi, O, and I elements are homogeneously distributed on the microspheres. Also, the elemental

composition analysis indicated that the empirical formula of the flower-like microspheres is Bi_3O_6I (Fig. 2g), which is similar to the reported chemical formula of $Bi_4O_5I_2$ [34].

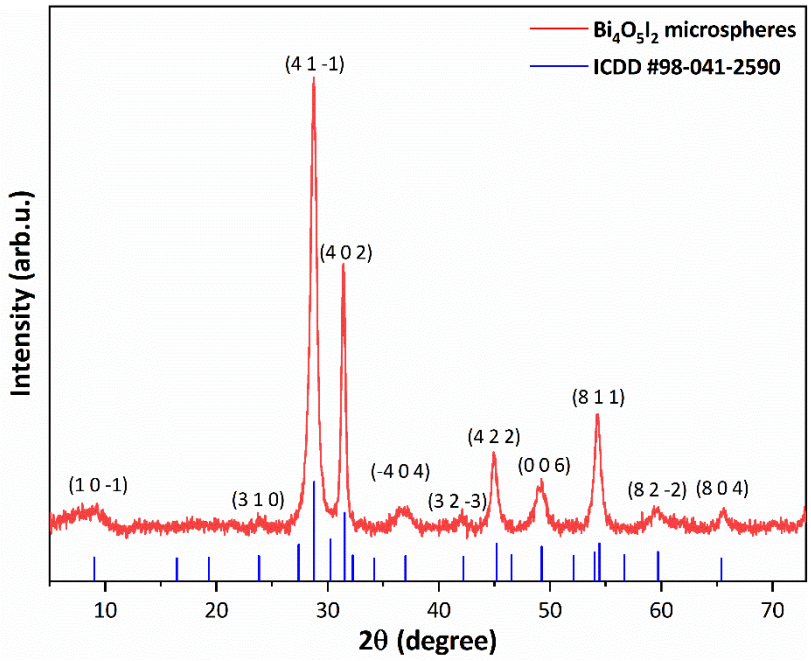

Figure 1. XRD patterns of $Bi_4O_5I_2$ flower-like microspheres.

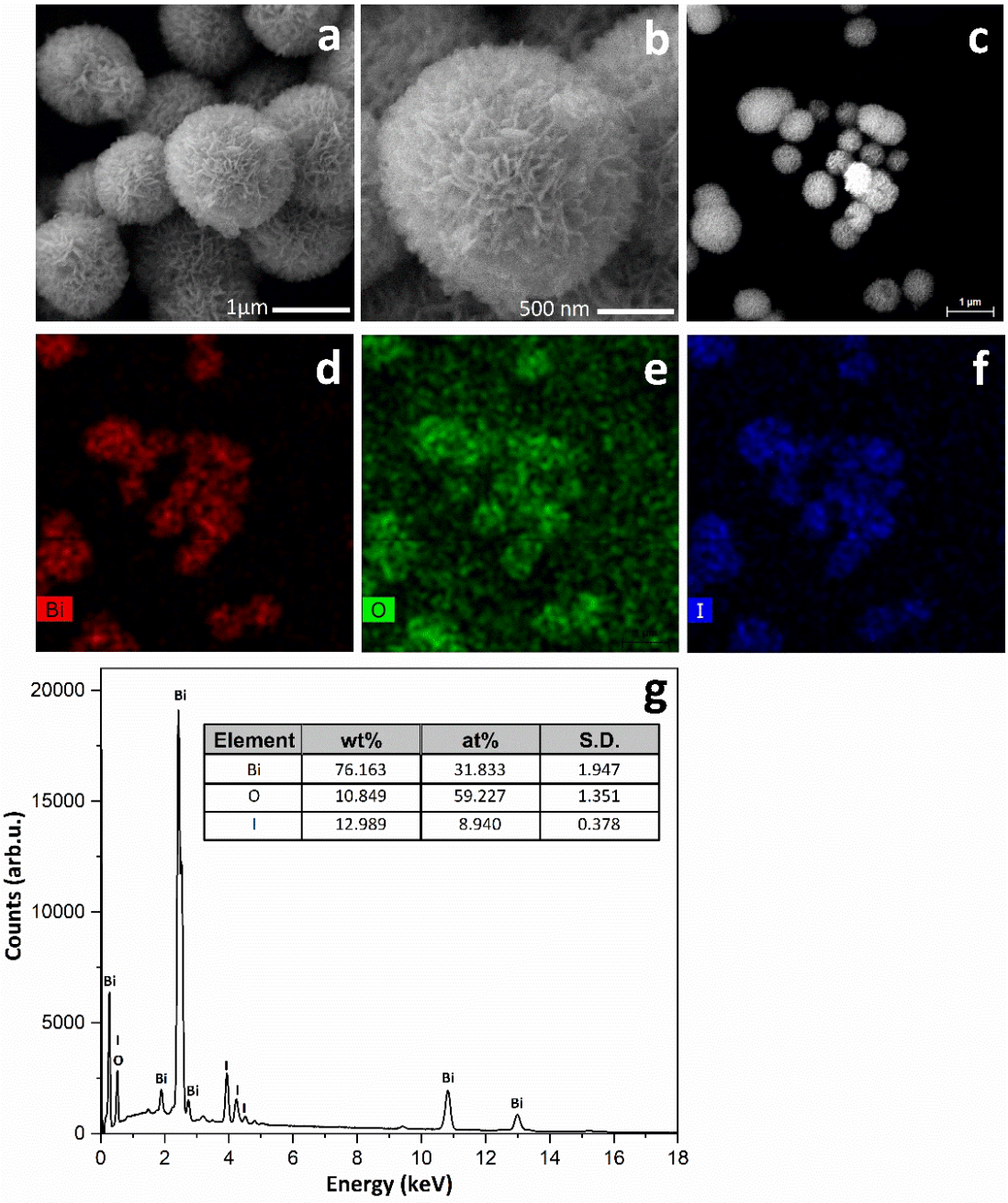

Figure 2. SEM images (a-b), mapping (c-f) and elemental analysis (g) by EDS of $Bi_4O_5I_2$ flower-like microspheres.

3.2. Photocatalytic degradation of propylparaben

The photocatalytic activity of $Bi_4O_5I_2$ microspheres was evaluated by degrading a solution of 5 mg L^{-1} of PP (Table S1). As seen in Fig. 3, the photolysis of PP by the light can be discarded because the concentration was constant during 4 hours. Moreover,

the adsorption of 5 mg L^{-1} of PP in dark conditions on the surface of $Bi_4O_5I_2$ microspheres was 1%. Therefore, the adsorption of PP was negligible due to the pollutant has neutral charge at pH 7.0, which is the pH of the solution used in this work [40]. In this case, the negligible adsorption of propylparaben is due to the zero electrostatic attraction between the neutrally charged molecule and the semiconductor surface with a possible charge [41]. Nevertheless, in the presence of $Bi_4O_5I_2$ microspheres and under visible light irradiation, the percentage of the remaining PP decreased from 99% to 3% (i.e., from 4.98 to 0.13 mg L^{-1}). Moreover, the degradation rate of PP never reached a stationary phase, suggesting that the surface of the $Bi_4O_5I_2$ microspheres has not been saturated with PP molecules and reaction by-products, during the photocatalytic process. The non-saturation of the active sites of the semiconductor surface during the photocatalytic process is important in order to degrade the remaining pollutant completely [42]. For example, Tu et al. [29] reported a micro/nano photocatalyst of $Bi_4O_5I_2$ unable to degrade more than 40% of a 10 mg L^{-1} PP solution, because the active sites of the surface might have been saturated with PP molecules and by-products, inhibiting the photocatalytic activity.

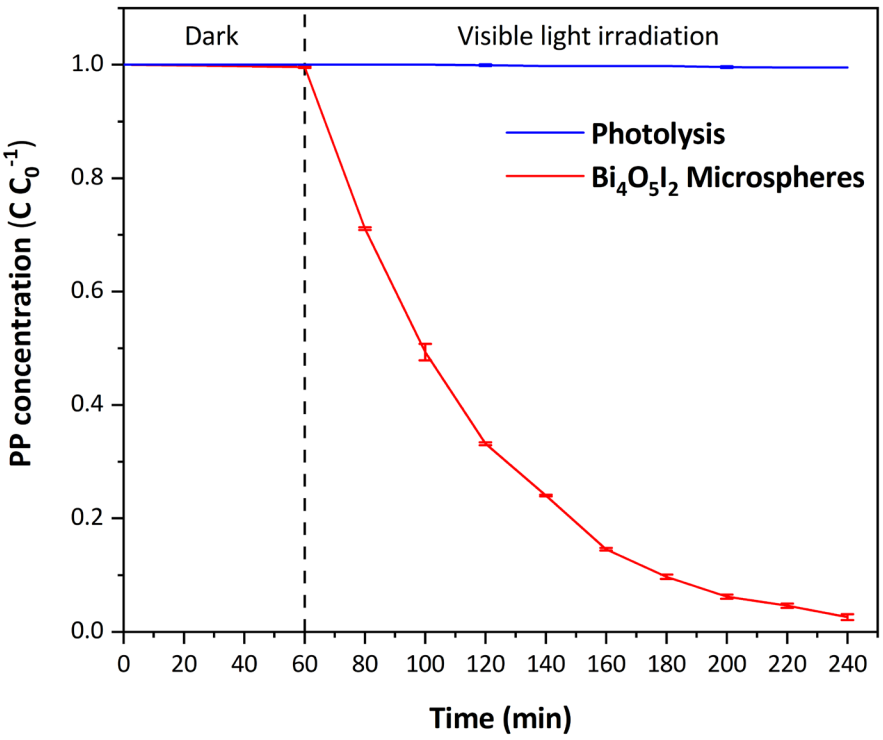

Figure 3. Photocatalytic degradation of PP by $Bi_4O_5I_2$ microspheres**.**

On the one hand, although, the time to degrade 97% of the PP was long, the efficiency of the microspheres can be considered high. This is because $Bi_4O_5I_2$ microspheres required a lamp with a lower power (50 W) than the lamps used in other works, for almost completely eliminate PP [29,43,44]. By increasing the intensity of the lamp allows a higher flux of photons toward the reactive center of the semiconductor, generating a higher amount of charge carriers, and therefore, speeding up the photocatalytic reaction [45]. However, in a reported work [29], $Bi_4O_5I_2$ micro/nano photocatalyst could only degrade 40% of the PP solution (10 mg L^{-1}) in 120 min even using a light source with an intensity of 1000 W. Likewise, the photocatalyst dosage for the degradation of PP in this work was 0.2857 g L^{-1}. This photocatalyst dosage can be considered low in comparison with several works of $Bi_xO_yX_z$ semiconductors, where it has been reported dosages of 1 g L^{-1} for the degradation of PP [17,29,44]. A photocatalytic process that requires a low dosage to completely eliminate a pollutant makes it more eligible for practical implementation in water treatment [46]. For these reasons, the $Bi_4O_5I_2$ microspheres reported in this work could be eligible as a photocatalyst for water purification.

3.3. Photocatalytic inactivation of *E. coli*

The photocatalytic inactivation of *E. coli* by $Bi_4O_5I_2$ microspheres is displayed in Fig. 4, Fig. S2, and Table S2. No decrease of viable cell density was observed in the negative control, suggesting that saline solution and visible light irradiation did not have a direct inactivation effect in *E. coli*, which is consistent with other studies [30,47,48]. As well as, in dark conditions and in presence of $Bi_4O_5I_2$ microspheres, the cell density did not drop, which indicates the non-toxicity of the photocatalyst on *E. coli* cells. Nevertheless, in presence of $Bi_4O_5I_2$ microspheres and under visible light irradiation, the cell density of *E. coli* cells decreased from $1.75x10^7$ to $1.4 x10^4$ CFU mL^{-1}.

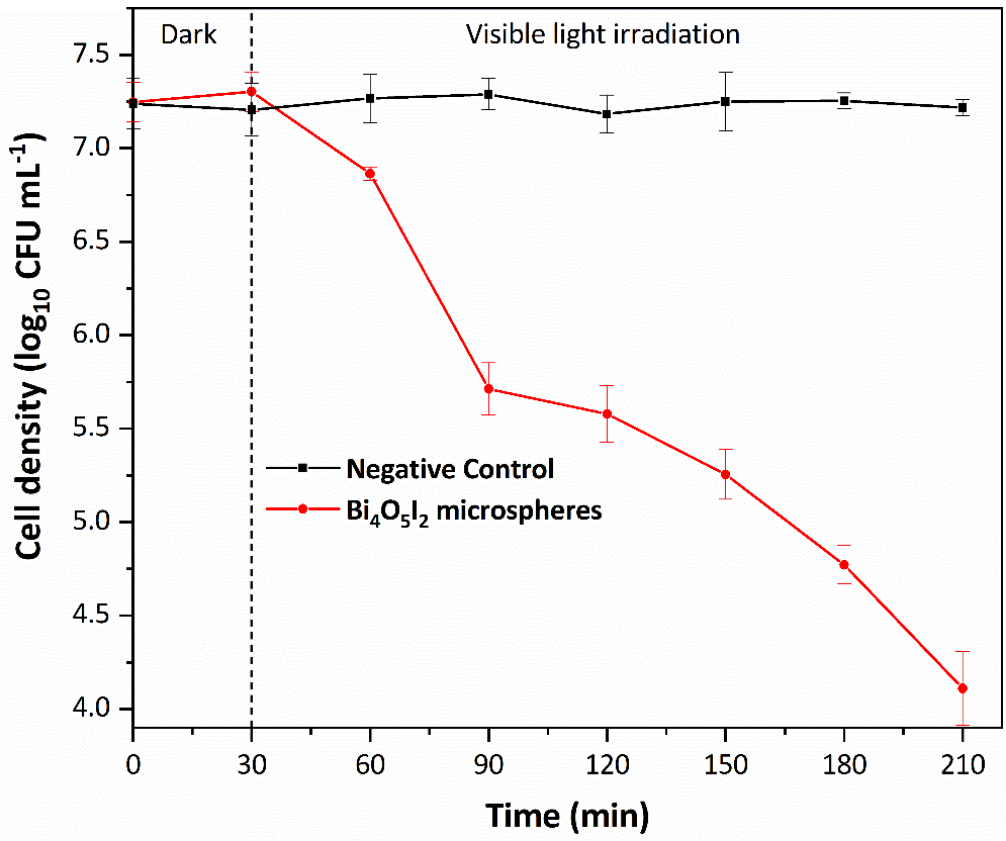

Figure 4. Photocatalytic inactivation of *E. Coli* by $Bi_4O_5I_2$ flower-like microspheres.

Furthermore, the behavior of the inactivation curve under visible light indicates that during the first 60 min the inactivation of *E. coli* was progressive. However, after 60 min of light irradiation there was a decrease in photocatalytic activity and, therefore, the inactivation of *E. coli* was slowed down. The reason for the temporal decrease is the high antioxidant defense of *E. coli* in the initial stages of inactivation [49]. Subsequently, after 90 min, there was again a progressive photocatalytic inactivation, suggesting deficiencies on the repair mechanisms of *E. coli* cells under ROS stress [19]. This is because a long exposure and accumulation of ROS (e.g., $^{\cdot}OH$) can unchain deficiencies and cause critical damage on the bacterial cells by lipid peroxidation (e.g., lipid radicals and lipid peroxyl radicals), protein oxidation (e.g., oxidation of Coenzyme A) and DNA breakage [19,50–52]. Therefore, these results suggest that $Bi_4O_5I_2$ microspheres might have an effective ROS production for the inactivation of *E. coli*.

4. CONCLUSIONS

$Bi_4O_5I_2$ flower-like microspheres were successfully synthesized by a solvothermal method, followed by calcination. The $Bi_4O_5I_2$ microspheres exhibited an excellent photocatalytic activity in the degradation of PP and inactivation of *E. coli* cells. On the one hand, $Bi_4O_5I_2$ microspheres were capable of almost degrade completely PP with a light source of 50 W, proving their high efficiency for the degradation of organic pollutants. On the other hand, although 43% of *E. coli* cells survived, the inactivation curve showed that the $Bi_4O_5I_2$ microspheres could completely inactivate *E. coli* cells if the photocatalytic test is performed for a longer time. Therefore, the results obtained in this research demonstrated that $Bi_4O_5I_2$ microspheres can be a suitable photocatalyst for degradation of pollutants and inactivation of gram-negative bacteria. Thus, these results suggest that $Bi_xO_yI_z$ photocatalysts could be a potential candidate for water treatment due to their high photocatalytic activity.

5. FUNDING SOURCES

This research was funded by Erasmus + CBHE consortium “Nature–based living lab for interdisciplinary practical and research semester on sustainable development and environmental protection in the amazon rainforest (Contract Number: 619346–EPP–1–2020–1–DE –EPPKA2–CBHE–JP).

6. AUTHOR CONTRIBUTIONS: CREDIT

Leonardo Proaño-Rhon: Conceptualization, Data curation, Methodology, Investigation, Writing – original draft. **Maria Auquilla-Villamagua:** Conceptualization, Data curation,

Methodology, Investigation. **Giovanna Morán-Marcillo:** Methodology, Investigation, Writing – review & editing. **Michael Zuarez-Chamba:** Conceptualization, Methodology, Investigation, Writing – review & editing. **Karla Vizuete:** Investigation, Writing – review & editing. **Alexis Debut:** Investigation, Writing – review & editing. **Miguel Quishpe:** Supervision, Funding acquisition, Writing – review & editing. **Miguel Herrera-Robledo:** Supervision, Funding acquisition, Writing – review & editing.

7. ACKNOWLEDGMENT

Thanks to CENCINAT of the Universidad de las Fuerzas Armadas ESPE for the characterization of the photocatalyst. Also, thanks to Molecular Biology Laboratory of Ikiam University for the support with bacterial strain and equipment for the development of the photocatalytic inactivation research. Finally, thanks to the Geosciences Laboratory for Research and Chemistry Laboratory of Ikiam for the support of workspace and materials.

8. REFERENCES

[1] United Nations Environment Programme and the World Health Organization, State of the Science of Endocrine Disrupting Chemicals - 2012, Geneva, 2013.

[2] J.E. Schjenken, E.S. Green, T.S. Overduin, C.Y. Mah, D.L. Russell, S.A. Robertson, Endocrine Disruptor Compounds—A Cause of Impaired Immune Tolerance Driving Inflammatory Disorders of Pregnancy?, Front Endocrinol (Lausanne) 12 (2021). https://doi.org/10.3389/fendo.2021.607539.

[3] L.N. Vandenberg, J. Bugos, Assessing the Public Health Implications of the Food Preservative Propylparaben: Has This Chemical Been Safely Used for Decades, Curr Environ Health Rep 8 (2021) 54–70. https://doi.org/10.1007/s40572-020-00300-6/Published.

[4] M.C. García-Espiñeira, L.P. Tejeda-Benítez, J. Olivero-Verbel, Toxic effects of bisphenol A, propyl paraben, and triclosan on caenorhabditis elegans, Int J Environ Res Public Health 15 (2018). https://doi.org/10.3390/ijerph15040684.

[5] A. Zgoła-Grześkowiak, M. Jeszka-Skowron, B. Czarczyńska-Goślińska, T. Grześkowiak, Determination of Parabens in Polish River and Lake Water as a Function of Season, Anal Lett 49 (2016) 1734–1747. https://doi.org/10.1080/00032719.2015.1120739.

[6] M. Becerra-Herrera, V. Miranda, P. Richter, Rapid determination of parabens in water samples by ultra-high performance liquid chromatography coupled to time of flight mass spectrometry, Analytical Sciences 36 (2020) 675–679. https://doi.org/10.2116/ANALSCI.19P409.

[7] A.F. Fransway, P.J. Fransway, D. V. Belsito, J.A. Yiannias, Paraben Toxicology, Dermatitis 30 (2019) 32–45. https://doi.org/10.1097/DER.0000000000000428.

[8] M.Y. Shin, C. Shin, J.W. Choi, J. Lee, S. Lee, S. Kim, Pharmacokinetic profile of propyl paraben in humans after oral administration, Environ Int 130 (2019). https://doi.org/10.1016/j.envint.2019.104917.

[9] H. Assaf Vandecasteele, F. Gautier, F. Tourneix, E. van Vliet, D. Bury, N. Alépée, Next generation risk assessment for skin sensitisation: A case study with propyl paraben, Regulatory Toxicology and Pharmacology 123 (2021). https://doi.org/10.1016/j.yrtph.2021.104936.

[10] P. Kovalakova, L. Cizmas, T.J. McDonald, B. Marsalek, M. Feng, V.K. Sharma, Occurrence and toxicity of antibiotics in the aquatic environment: A review, Chemosphere 251 (2020) 126351. https://doi.org/10.1016/J.CHEMOSPHERE.2020.126351.

[11] World Health Organization, Global Antimicrobial Resistance and Use Surveillance System (GLASS) Report 2022, 2022. https://www.who.int/publications/book-orders.

[12] M.A. Abushaheen, Muzaheed, A.J. Fatani, M. Alosaimi, W. Mansy, M. George, S. Acharya, S. Rathod, D.D. Divakar, C. Jhugroo, S. Vellappally, A.A. Khan, J. Shaik, P. Jhugroo, Antimicrobial

resistance, mechanisms and its clinical significance, Disease-a-Month 66 (2020). https://doi.org/10.1016/j.disamonth.2020.100971.

[13] World Health Organization, Water, Sanitation, Hygiene and Health a Primer for Health Professionals, Geneva, 2019.

[14] V.S. Braz, K. Melchior, C.G. Moreira, Escherichia coli as a Multifaceted Pathogenic and Versatile Bacterium, Front Cell Infect Microbiol 10 (2020). https://doi.org/10.3389/fcimb.2020.548492.

[15] E. Denamur, O. Clermont, S. Bonacorsi, D. Gordon, The population genetics of pathogenic Escherichia coli, Nature Research, 2021. https://doi.org/10.1038/s41579-020-0416-x.

[16] Z. hua Liu, Y. Kanjo, S. Mizutani, Removal mechanisms for endocrine disrupting compounds (EDCs) in wastewater treatment - physical means, biodegradation, and chemical advanced oxidation: A review, Science of the Total Environment 407 (2009) 731–748. https://doi.org/10.1016/j.scitotenv.2008.08.039.

[17] V.H. Nguyen, L.A. Phan Thi, P.S. Chandana, H.T. Do, T.H. Pham, T. Lee, T.D. Nguyen, C. Le Phuoc, P.T. Huong, The degradation of paraben preservatives: Recent progress and sustainable approaches toward photocatalysis, Chemosphere 276 (2021). https://doi.org/10.1016/j.chemosphere.2021.130163.

[18] A.L. Srivastav, N. Patel, V.K. Chaudhary, Disinfection by-products in drinking water: Occurrence, toxicity and abatement, Environmental Pollution 267 (2020). https://doi.org/10.1016/j.envpol.2020.115474.

[19] M. Wang, M. Ateia, D. Awfa, C. Yoshimura, Regrowth of bacteria after light-based disinfection — What we know and where we go from here, Chemosphere 268 (2021). https://doi.org/10.1016/j.chemosphere.2020.128850.

[20] S.S. Shekhawat, N.M. Kulshreshtha, V. Vivekanand, A.B. Gupta, Impact of combined chlorine and UV technology on the bacterial diversity, antibiotic resistance genes and disinfection by-products in treated sewage, Bioresour Technol 339 (2021). https://doi.org/10.1016/j.biortech.2021.125615.

[21] M.A. Gondal, C. Xiaofeng, M.A. Dastageer, Advanced Structured Materials Novel Bismuth-Oxyhalide-Based Materials and Their Applications, New Delhi, 2017. https://doi.org/10.1007/978-81-322-3739-6.

[22] M. Zuarez-Chamba, S. Rajendran, M. Herrera-Robledo, A.K. Priya, C. Navas-Cárdenas, Bi-based photocatalysts for bacterial inactivation in water: Inactivation mechanisms, challenges, and strategies to improve the photocatalytic activity, Environ Res 209 (2022). https://doi.org/10.1016/j.envres.2022.112834.

[23] A. Hernández-Ramírez, I. Medina-Ramírez, Semiconducting materials, in: Photocatalytic Semiconductors: Synthesis, Characterization, and Environmental Applications, Springer International Publishing, 2015: pp. 1–40. https://doi.org/10.1007/978-3-319-10999-2_1.

[24] M.E. Simonsen, Heterogeneous Photocatalysis, in: Chemistry of Advanced Environmental

Purification Processes of Water: Fundamentals and Applications, Elsevier Inc., 2014: pp. 135–170. https://doi.org/10.1016/B978-0-444-53178-0.00004-3.

[25] X. Jin, L. Ye, H. Xie, G. Chen, Bismuth-rich bismuth oxyhalides for environmental and energy photocatalysis, Coord Chem Rev 349 (2017) 84–101. https://doi.org/10.1016/j.ccr.2017.08.010.

[26] P.S. Basavarajappa, S.B. Patil, N. Ganganagappa, K.R. Reddy, A. V. Raghu, C.V. Reddy, Recent progress in metal-doped TiO2, non-metal doped/codoped TiO2 and TiO2 nanostructured hybrids for enhanced photocatalysis, Int J Hydrogen Energy 45 (2020) 7764–7778. https://doi.org/10.1016/j.ijhydene.2019.07.241.

[27] N.B. McGuinness, M. Garvey, A. Whelan, H. John, C. Zhao, G. Zhang, D.D. Dionysiou, J.A. Byrne, S.C. Pillai, Nanotechnology Solutions for Global Water Challenges, in: ACS Symposium Series, American Chemical Society, 2015: pp. 375–411. https://doi.org/10.1021/bk-2015-1206.ch018.

[28] M. Zuarez-Chamba, D. Tuba-Guamán, M. Quishpe, K. Pazmiño, K. Vizuete, A. Debut, P.A. Cisneros-Pérez, C. Reinoso, C. Santacruz, A. Salgado, C.R. Arroyo, P. Iza, N. Miguel, Z. Niño-Ruiz, M. Herrera-Robledo, Synthesis of Bi4O5I2 microbars for pollutant degradation through a photocatalytic process, Mater Lett 336 (2023). https://doi.org/10.1016/j.matlet.2023.133888.

[29] S. Tu, M. Lu, X. Xiao, C. Zheng, H. Zhong, X. Zuo, J. Nan, Flower-like Bi4O5I2/Bi5O7I nanocomposite: Facile hydrothermal synthesis and efficient photocatalytic degradation of propylparaben under visible-light irradiation, RSC Adv 6 (2016) 44552–44560. https://doi.org/10.1039/c6ra03988j.

[30] Z. Ma, N. Wang, W. Guo, K. Zhang, J. Li, Synthesis of Bi4O5I2 for bacterial inactivation with visible light exposure, Mater Lett 352 (2023) 135207. https://doi.org/10.1016/j.matlet.2023.135207.

[31] M. Lan, N. Zheng, X. Dong, C. Hua, H. Ma, X. Zhang, Bismuth-rich bismuth oxyiodide microspheres with abundant oxygen vacancies as an efficient photocatalyst for nitrogen fixation, Dalton Transactions 49 (2020) 9123–9129. https://doi.org/10.1039/d0dt01332c.

[32] P. Yang, Z. Li, J. Zhong, S. Huang, J. Li, Study on phase transformation of BiOI and corresponding photocatalytic activity, Solid State Sci 147 (2024). https://doi.org/10.1016/j.solidstatesciences.2023.107387.

[33] M. Zuarez-Chamba, D. Tuba-Guamán, M. Quishpe, K. Vizuete, A. Debut, M. Herrera-Robledo, Photocatalytic degradation of bisphenol A on BiOI nanostructured films under visible LED light irradiation, J Photochem Photobiol A Chem 431 (2022). https://doi.org/10.1016/j.jphotochem.2022.114021.

[34] E. Keller, V. Krämer, M. Schmidt Ii, H. Oppermann, The crystal structure of Bi 4 O 5 I 2 and its relation to the structure of Bi 4 O 5 Br 2, Z Kristallogr Cryst Mater 217 (2002) 256–264.

[35] X. Xiao, C. Xing, G. He, X. Zuo, J. Nan, L. Wang, Solvothermal synthesis of novel hierarchical Bi4O5I2 nanoflakes with highly visible light photocatalytic performance for the degradation of 4-tert-butylphenol, Appl Catal B 148–149 (2014) 154–163. https://doi.org/10.1016/j.apcatb.2013.10.055.

[36] H. Zhang, X. Zhang, Z. Zhang, X. Ma, Y. Zhu, M. Ren, Y. Cao, P. Yang, Ultrahigh Charge Separation

Achieved by Selective Growth of Bi4O5I2Nanoplates on Electron-Accumulating Facets of Bi5O7I Nanobelts, ACS Appl Mater Interfaces 13 (2021) 39985–40001. https://doi.org/10.1021/acsami.1c06188.

[37] L. Zhang, T. Zhai, M. Yang, C. Hu, Few-layered Bi4O5I2 nanosheets enclosed by {1 0−1} facets with oxygen vacancies for highly-efficient removal of water contaminants, J Hazard Mater 437 (2022). https://doi.org/10.1016/j.jhazmat.2022.129274.

[38] J. Wei, S. Xue, P. Xie, R. Zou, Synthesis and photocatalytic properties of different SnO 2 microspheres on graphene oxide sheets, Appl Surf Sci 376 (2016) 172–179. https://doi.org/10.1016/j.apsusc.2016.03.058.

[39] W. Jiang, Y. Zhu, G. Zhu, Z. Zhang, X. Chen, W. Yao, Three-dimensional photocatalysts with a network structure, J Mater Chem A Mater 5 (2017) 5661–5679. https://doi.org/10.1039/c7ta00398f.

[40] Y. Wei, X. Liu, Z. Wang, Y. Chi, T. Yue, Y. Dai, J. Zhao, B. Xing, Adsorption and catalytic degradation of preservative parabens by graphene-family nanomaterials, Science of the Total Environment 806 (2022). https://doi.org/10.1016/j.scitotenv.2021.150520.

[41] R. Gusain, K. Gupta, P. Joshi, O.P. Khatri, Adsorptive removal and photocatalytic degradation of organic pollutants using metal oxides and their composites: A comprehensive review, Adv Colloid Interface Sci 272 (2019) 102009. https://doi.org/10.1016/J.CIS.2019.102009.

[42] D.E. Lee, M.K. Kim, M. Danish, W.K. Jo, State-of-the-art review on photocatalysis for efficient wastewater treatment: Attractive approach in photocatalyst design and parameters affecting the photocatalytic degradation, Catal Commun 183 (2023). https://doi.org/10.1016/j.catcom.2023.106764.

[43] H. Fang, Y. Gao, G. Li, J. An, P.K. Wong, H. Fu, S. Yao, X. Nie, T. An, Advanced oxidation kinetics and mechanism of preservative propylparaben degradation in aqueous suspension of TiO2 and risk assessment of its degradation products, Environ Sci Technol 47 (2013) 2704–2712. https://doi.org/10.1021/es304898r.

[44] X. Xiao, M. Lu, J. Nan, X. Zuo, W. Zhang, S. Liu, S. Wang, Rapid microwave synthesis of I-doped Bi4O5Br2 with significantly enhanced visible-light photocatalysis for degradation of multiple parabens, Appl Catal B 218 (2017) 398–408. https://doi.org/10.1016/j.apcatb.2017.06.074.

[45] H.Q. Xiong, H.R. Bao, F. Long, Y.Y. Du, J.Z. Qu, Z.X. Luan, X.L. Sun, From lab to nature: Overcoming challenges in applying in-situ photocatalysis to water bodies, J Environ Chem Eng 12 (2024). https://doi.org/10.1016/j.jece.2024.112656.

[46] M.A. Al-Nuaim, A.A. Alwasiti, Z.Y. Shnain, The photocatalytic process in the treatment of polluted water, Chemical Papers 77 (2023) 677–701. https://doi.org/10.1007/s11696-022-02468-7.

[47] Y. Zhou, M. Gao, R. Liu, Z. Zhang, X. Tang, Preparation and antibacterial properties of bismuth-rich Bi/Bi4O5I2 photocatalytic materials with surface defects, Colloids Surf A Physicochem Eng Asp 671 (2023) 131627. https://doi.org/10.1016/J.COLSURFA.2023.131627.

[48] Y. Long, Y. Wang, D. Zhang, P. Ju, Y. Sun, Facile synthesis of BiOI in hierarchical nanostructure preparation and its photocatalytic application to organic dye removal and biocidal effect of bacteria, J Colloid Interface Sci 481 (2016) 47–56. https://doi.org/10.1016/j.jcis.2016.07.041.

[49] J. Ma, Y. Shi, D. An, Y. Chen, J. Guo, Y. Qian, S. Wang, J. Lu, Inactivation mechanism of E. coli in water by enhanced photocatalysis under visible light irradiation, Science of the Total Environment 866 (2023). https://doi.org/10.1016/j.scitotenv.2023.161450.

[50] I. Michael-Kordatou, P. Karaolia, D. Fatta-Kassinos, The role of operating parameters and oxidative damage mechanisms of advanced chemical oxidation processes in the combat against antibiotic-resistant bacteria and resistance genes present in urban wastewater, Water Res 129 (2018) 208–230. https://doi.org/10.1016/j.watres.2017.10.007.

[51] R. Gupta, J. Modak, Bacterial Lysis via Photocatalysis - A Critical Mechanistic Review, ChemCatChem 12 (2020) 2148–2170. https://doi.org/10.1002/cctc.201901831.

[52] Y. Hong, J. Zeng, X. Wang, K. Drlica, X. Zhao, Post-stress bacterial cell death mediated by reactive oxygen species, Proc Natl Acad Sci U S A 116 (2019) 10064–10071. https://doi.org/10.1073/pnas.1901730116.

9. SUPPLEMENTARY MATERIAL

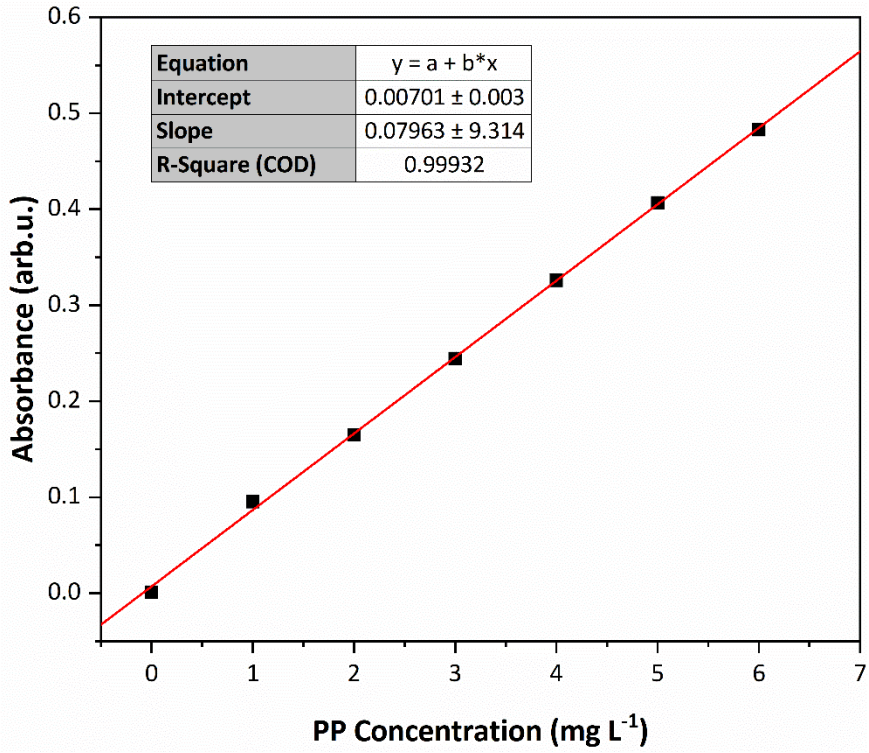

Figure S1. Calibration curve for determine the PP concentration.

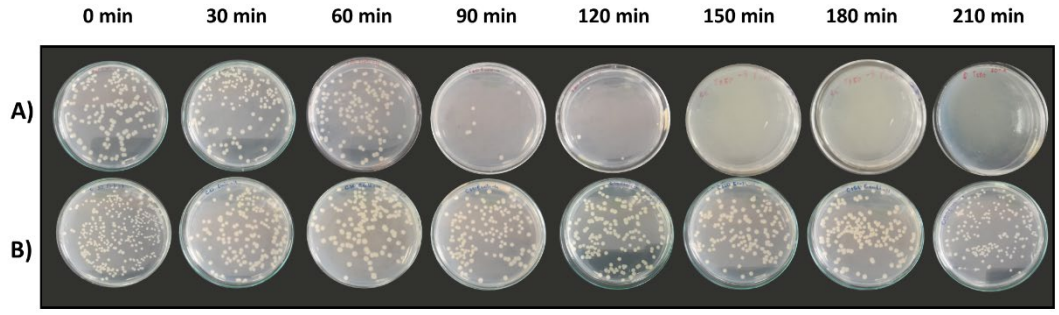

Figure S2. Photographs of the A) photocatalytic inactivation of *E. coli* colonies by $Bi_4O_5I_2$ microspheres and B) the negative control in the assay.

Table S1. Statistical analysis of the PP degradation by $Bi_4O_5I_2$ microspheres.

	Photolysis		$Bi_4O_5I_2$ microspheres	
Time (min)	**PP concentration ($C\ C_0^{-1}$)**	**Standard deviation ($C\ C_0^{-1}$)**	**PP concentration ($C\ C_0^{-1}$)**	**Standard deviation ($C\ C_0^{-1}$)**
0	1	0	1	0
60	1	0	0.995	0.001
80	1	0	0.711	0.002
100	1	0	0.493	0.014
120	0.999	0.001	0.331	0.002
140	0.997	0	0.240	0.001
160	0.997	0	0.146	0.002
180	0.997	0	0.097	0.003
200	0.996	0.001	0.061	0.003
220	0.995	0	0.046	0.003
240	0.995	0	0.025	0.005

Table S2. Statistical analysis of the inactivation of *E. coli* by $Bi_4O_5I_2$ microspheres.

	Negative control		$Bi_4O_5I_2$ microspheres	
Time (min)	***E. coli* cell density (log_{10} CFU mL^{-1})**	**Standard deviation (log_{10} CFU mL^{-1})**	***E. coli* cell density (log_{10} CFU mL^{-1})**	**Standard deviation (log_{10} CFU mL^{-1})**
0	7.238	0.133	7.246	0.106
30	7.205	0.141	7.303	0.105
60	7.267	0.129	6.864	0.036
90	7.288	0.084	5.712	0.14
120	7.184	0.101	5.579	0.151
150	7.251	0.157	5.256	0.133
180	7.254	0.041	4.772	0.101
210	7.217	0.04106	4.110	0.199